Photonic Crystals

International Edition: DOI: 10.1002/anie.201502268
German Edition: DOI: 10.1002/ange.201502268

The Mechanism of Color Change in the Neon Tetra Fish: a Light-Induced Tunable Photonic Crystal Array**

*Dvir Gur, Benjamin A. Palmer, Ben Leshem, Dan Oron, Peter Fratzl, Steve Weiner, and Lia Addadi**

Abstract: *The fresh water fish neon tetra has the ability to change the structural color of its lateral stripe in response to a change in the light conditions, from blue-green in the light-adapted state to indigo in the dark-adapted state. The colors are produced by constructive interference of light reflected from stacks of intracellular guanine crystals, forming tunable photonic crystal arrays. We have used micro X-ray diffraction to track in time distinct diffraction spots corresponding to individual crystal arrays within a single cell during the color change. We demonstrate that reversible variations in crystal tilt within individual arrays are responsible for the light-induced color variations. These results settle a long-standing debate between the two proposed models, the "Venetian blinds" model and the "accordion" model. The insight gained from this biogenic light-induced photonic tunable system may provide inspiration for the design of artificial optical tunable systems.*

In animals colors are produced either by pigment coloration[1] or by structural colors.[2] Many animal taxa have independently evolved strategies to produce structural colors using 2D or 3D arrays of various materials, including chitin[3] and cellulose fibers,[4] calcite,[5] and guanine crystals. Optical systems based on intracellular arrays of thin guanine crystal platelets intercalated with cytoplasm are found in a variety of marine and terrestrial animals, such as fish, copepods, crabs, chameleons, and spiders.[6]

When light interacts with structures consisting of alternating layers of two materials with different refractive indices (n), the reflected light undergoes constructive interference for some wavelengths and destructive interference for others. Such a multilayer array acts as a reflector when the optical thicknesses nd (the product of the physical thicknesses d_l, d_h and the respective refractive indices n_l, n_h) of all layers are comparable to the wavelength of light, resulting in distinct colors being observed.[6b,7] Large index contrasts Δn provide increased reflectivity with fewer dielectric layers.[7a] The widespread use of guanine crystals in a variety of systems is probably due to its exceptionally high refractive index, $n = 1.83$, along the axis normal to the biogenic platelet crystals. The large plate faces are parallel to the (102) crystallographic plane of anhydrous guanine ($P_{2_1/c}$ $a = 3.55$, $b = 9.69$, $c = 16.35$ Å, $\beta = 95.88°$).[8] The refractive index of the cytoplasm is $n = 1.33$, thus providing a high-index contrast.

In most systems the spacings of guanine crystals and cytoplasm are fixed, but there are a few known cases in which the spacings change when triggered by appropriate signals.[9] One of the most striking examples is the neon tetra fish, which use changes in spacing to modify the structural color of its lateral stripe from blue-green ($\lambda \approx 490$ nm) to indigo ($\lambda \approx 400$ nm) in response to different light stimuli[10] (Figure 2a and movie S1 in the Supporting Information, SI). Previous studies reported a variety of different thicknesses for the guanine crystals ranging from 5–60 nm.[6a,11] The thickness of the cytoplasm spacings was never reported. In theoretical models used to simulate the reflectance properties, the cytoplasm thickness was adjusted to produce the observed reflected color by constructive interference.[11b,c,12] Lythgoe and Shand suggested that the variation in the spacing between the crystals is triggered by a change in osmotic pressure.[10,11c] Influx of water into the iridophores, the specialized cells containing guanine crystals, would lead to swelling of the iridophore cells with subsequent increase in crystal spacing, the "accordion" model.

In contrast, Nagaishi et al., and later Yoshioka et al., suggested that a controlled variation of the tilt angles of the single crystal platelets within the arrays leads to a change in platelet spacing; the so-called "Venetian blind" model.[11a,b,12] We used micro X-ray diffraction to resolve this ongoing

[*] D. Gur, Dr. B. A. Palmer, Prof. S. Weiner, Prof. L. Addadi
Department of Structural Biology
Weizmann Institute of Science
Rehovot, 76100 (Israel)
E-mail: lia.addadi@weizmann.ac.il
B. Leshem, Prof. D. Oron
Department of Physics of Complex Systems Institution
Weizmann Institute of Science
Rehovot, 76100, (Israel)
Prof. P. Fratzl
Department of Biomaterials
Max Planck Institute of Colloids and Interfaces
14424 Potsdam (Germany)

[**] We thank Yael Politi, Chenghao Lee, Stefan Siegel, and Ivo Zizak for help with the diffraction measurements at the μ-Spot beamline, in the synchrotron radiation facility BESSY-II. We thank the Irving and Cherna Moskowitz Center for Nano and Bio-Nano Imaging, the Weizmann Institute of Science, and in particular Eyal Shimoni, for support in the cryo-SEM imaging experiments. L.A. is the incumbent of the Dorothy and Patrick Gorman Professorial Chair of Biological Ultrastructure, and S.W. is the incumbent of the Dr. Trude Burchardt Professorial Chair of Structural Biology. This research was supported by a grant from the Israel Science foundation (grant no. 2012\224330*) and by a German Research Foundation grant within the framework of the Deutsch-Israelische Projektkooperation. The research leading to these results has received funding from the European Community's Seventh Framework Programme (FP7/2007-2013) under BioStruct-X (grant agreement no. 283570).

Supporting information for this article is available on the WWW under http://dx.doi.org/10.1002/anie.201502268.

debate, because the two mechanisms may be distinguished by monitoring the variation in the crystal orientation or absence thereof during the color change. This approach provides the possibility to track in time distinct diffraction points corresponding to the crystal array within a single iridophore, during the color change (Figure S1). If the crystal platelets change their orientation following the "Venetian blind" hypothesis, the azimuthal angle ω of the crystal diffraction will rotate by the amount $\Delta\omega$ (Figure 1a). In contrast, if the distance between the crystals changes because of swelling, but their relative tilt angle remains constant, the azimuth of the aligned

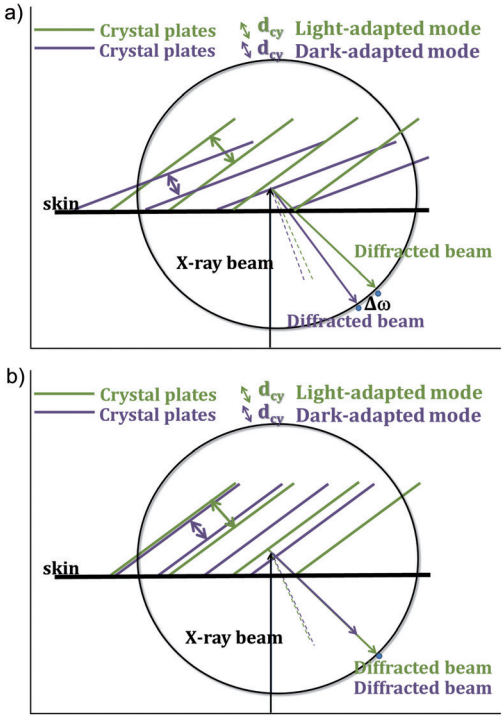

Figure 1. Schematic representation of the two mechanisms, and of the relative expected diffraction behavior: a) Change in crystal orientation following the "Venetian blind" model. b) Following the osmotic pressure model, the orientation is unchanged. The circle represents the diffraction that would be obtained from the planes parallel to the main face in randomly oriented crystal platelets. The blue dots represent the azimuthal position ω of the diffraction spots at the different specific crystal orientations represented. For reasons of clarity, the diffraction is presented in the reflection mode geometry.

crystal diffraction will remain unchanged (Figure 1b). To pursue this idea we first had to make sure that a section of the fish tissue containing the lateral stripe remains responsive to changes in light stimuli. Figure 2a shows a dissected lateral stripe immersed in physiological buffer: the lateral stripe is physiologically active under these conditions, and changes its color through several cycles of light and darkness.

We then used cryo-SEM to visualize the structural organization of the crystals within the iridophores. The iridophore cells are located just ventral to the mineralized collagenous scales. In a section transversal to the lateral stripe the majority of the crystal stacks are oriented edge on to the section, with a tilt of approximately 30° to the surface of the

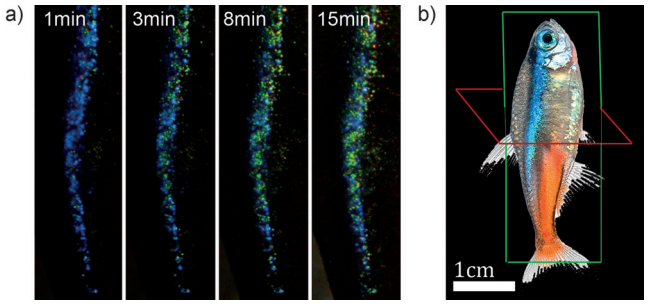

Figure 2. a) Optical images of the lateral stripe of the neon tetra. After 1 h of dark adaption the lateral stripe is violet-indigo. Stimulated by the exposure to bright light, it changes color to blue-green. After 15 min most of the transformation is complete. b) Image of a light-adapted fish with schematic representation of the transversal (red) and longitudinal (green) sections of the stripe.

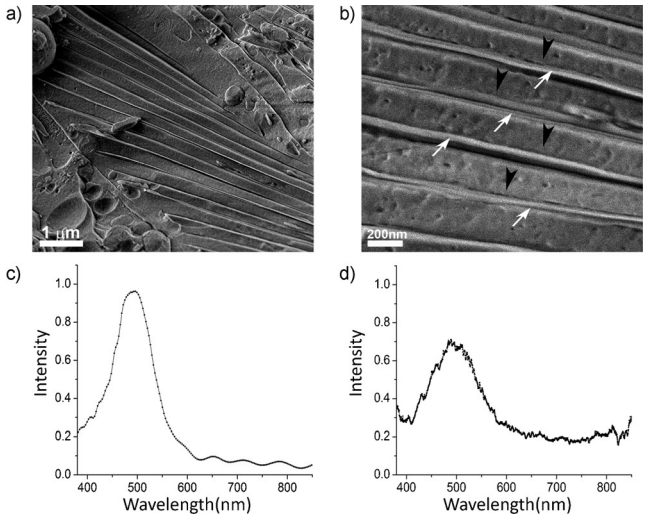

Figure 3. Light-adapted neon tetra: a,b) Cryo-SEM images of a guanophore located in the lateral stripe of the neon tetra, in a section transversal to the stripe. The guanophores are packed with ca. 20 nm thick crystals separated by thicker cytoplasm layers (white arrows, crystals; black arrow head, cytoplasm). c) Simulated reflectance based on the parameters measured in the cryo-SEM. d) Measured reflectance.

fish skin (Figure 3a,b), and with some variation in the orientation of crystal stacks among different iridophores. The crystals are arranged in ordered arrays of 20–30 alternating layers of thin guanine crystal (102) plates and thicker cytoplasm spacings (Figure 3a,b). The thickness of both the crystals and cytoplasm spacings of the light-adapted lateral stripe are quite uniform, 22 ± 4 nm ($n = 157$) and 155 ± 11 nm ($n = 125$), respectively. The thickness of the guanine crystals is comparable to that observed in other fish.[13] In contrast, the variability in cytoplasm spacings is much lower than that observed in fish scales, in which the relative disorder causes the broadband reflection and silver color.[6c,13] Taking into account the spacings of the crystal/cytoplasm layers measured from cryo-SEM micrographs, we simulated the reflectance spectrum using a Monte Carlo transfer matrix calculation (SI). The simulated reflectance resulted in a peak at about 490 nm (Figure 3d), which is in very good agreement

with the measured reflectance of the light-adapted state (Figure 3c). We note that the crystals are not completely parallel to each other: this both reduces and broadens the peak reflectance, as is indeed observed when comparing the simulated and measured reflectance.

Utilizing the information from the cryo-SEM, we then proceeded to design the wide-angle X-ray scattering experiment (WAXS) in a manner that will allow us to determine whether or not there is a change in crystal orientation that correlates with the color change. Ideally we would focus on the (102) reflection of the crystal platelets, which would directly monitor the change in orientation of the (102) platelets ($\Delta\omega$ in Figure 1a). However, sectioning and embedding, required to obtain the transverse sections in which the (102) platelets are in diffraction position (as in Figure 3), would compromise the integrity of the tissue and its ability to remain physiologically active and responsive to changes in the light conditions. We were thus forced to use longitudinal sections with the incident X-ray beam parallel to the incident light on the fish skin (Figure 4), in the same orientation as shown in Figure 2. Using this experimental set up, the (102) platelet reflection is not in diffracting position. We thus chose to monitor the (012) diffraction planes, which is in diffraction position in this orientation, and has the second highest intensity after the (102) planes (Figure 4). With this geometrical set-up, if the platelet tilt angle changes following light stimuli as in the "Venetian blind" model, depending on their orientation relative to the skin there will be stacks for which the (012) planes enter and go out of diffraction and stacks (few) that remain in diffraction throughout the whole cycle.

The experimental setup was as follows: thin sections obtained from the lateral stripe of the neon tetra were placed

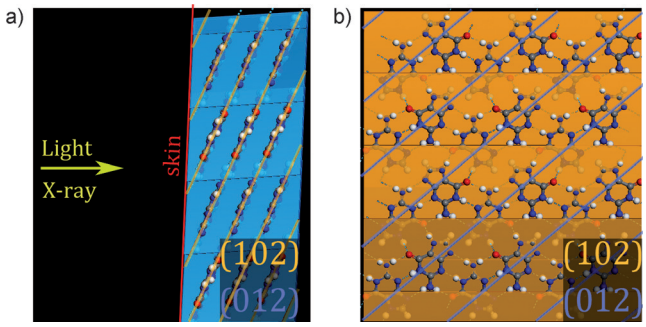

Figure 4. The crystal structure of anhydrous guanine, showing the (102) plane (orange) and the (012) plane (blue). The dihedral angle between the two planes is 68.7°. a) View along the *b* axis: The crystal (102) plates are edge on to the direction of view. The platelet orientation relative to the fish skin, as well as relative to the incident light and X-ray is indicated; b) View along the *a* axis: the (012) planes are edge-on to the direction of view. This is the geometry adopted in the diffraction experiment, with the X-ray beam coinciding with the direction of view.

under the X-ray beam in a light-adapted state while immersed in a buffer that allowed the cells to remain physiologically active throughout the whole experiment. WAXS patterns were collected at 60 s intervals for up to 2 h, while changing the light conditions. Individual diffraction spots were monitored through a full cycle of alternating light stimulations (light–dark–light).

The results of a full cycle (light–dark–light), in which the (012) reflection moved back and forth in response to dark and light conditions is shown in Figure 5 and in Video S2. The (012) plane is shifted by an azimuthal angle $\Delta\omega$ of about 3° counterclockwise when light was switched off (9–51 min), and about 3° clockwise when light was turned back on (91–

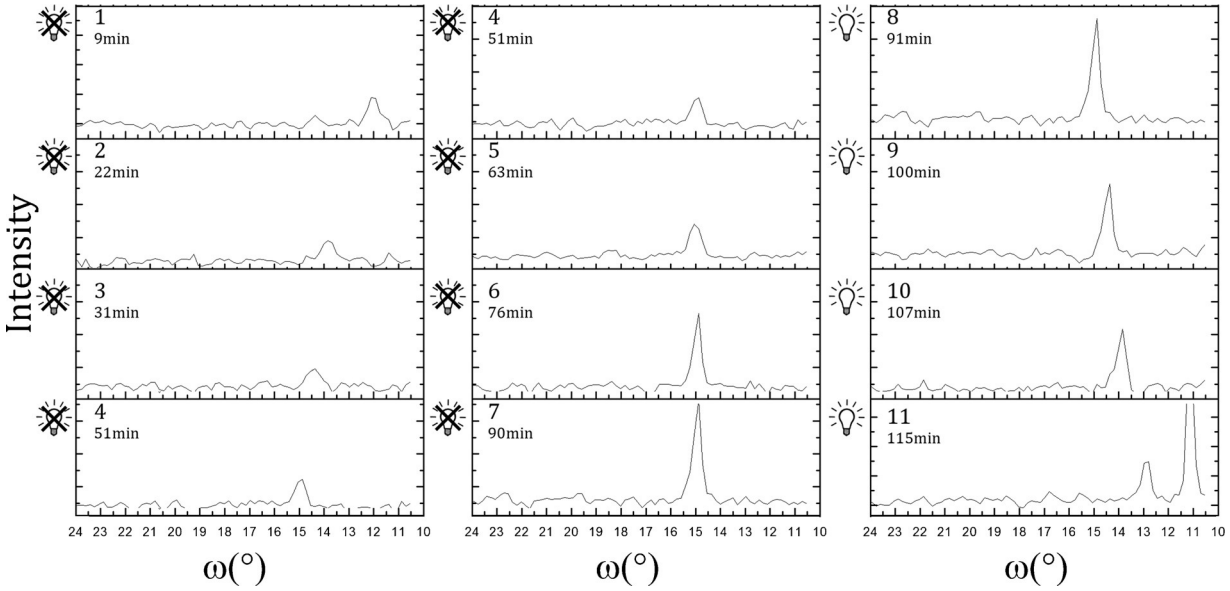

Figure 5. One individual diffraction spot monitored through a full cycle of alternating light stimulations (light–dark–light). Diffraction patterns were acquired every 60 s with a total of 115 patterns. The sample was kept under bright light prior to the experiment, then the lights were turned off and the measurement was started. A shift in the azimuth ω of the (012) anhydrous guanine crystal plane followed the change in the light conditions. The ω shifted counterclockwise when the lights were switched off (9–51 min), and clockwise when the lights were turned on (91–115 min). The ω remained constant after the tissue had adjusted to the light conditions (51–90 min). The increased peak amplitude in the later stages of the experiment is probably due to slight changes in the sampling location during the measurements.

115 min). Between the two cycles, the angle ω remained unchanged, as the tissue was fully adjusted to the light conditions (51–90 min). Two such complete cycles were observed. We also documented tens of cases when a shift of the diffraction spots of 1.5–3.3° was observed in response to a change in the light stimulation, after which the diffraction peak disappeared. This occurred when the crystal stacks were initially edge-on to the X-ray beam, but the light induced a tilt around an axis that was not parallel to the beam, removing them from diffraction orientation. Fifteen of these instances are summarized in Figure 6b, together with one such time-dependent series (Figure 6a).

a)

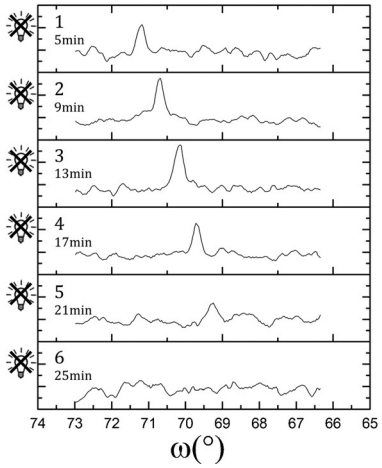

b)

Sample #	Δw(°)	Time of scan (min)
1	3.1	20
2	2.6	24
3	2.9	16
4	3.3	26
5	2.1	25
6	1.7	19
7	2.0	14
8	2.0	18
9	2.5	18
10	3.1	21
11	3.1	24
12	2.7	19
13	2.8	21
14	2.5	17
15	1.9	17

Figure 6. Examples of diffraction spots that disappeared after shifting during the light cycle. a) Radially integrated diffraction patterns of one individual diffraction spot in the same experiment as in Figure 5. The ω of the (012) anhydrous guanine crystal plane shifted when the light was turned off, and the diffraction peak disappeared after a shift of 2.1°. b) Table showing the $\Delta\omega$ [°] of a series of (012) diffraction spots observed in five different fish. The diffraction spots moved in a consistent manner in response to a change in light stimulation, until the diffraction peaks disappeared, when the (012) plane went out of diffraction position. Sample #5 corresponds to the diffraction spot monitored in (a).

These observations clearly indicate that the color change of the lateral stripe of the neon tetra is accompanied by a change in the tilt angle of the crystals, supporting the "Venetian blind" model proposed by Nagaishi et al.[11a,b] The structural parameters that were derived from cryo-SEM require the cytoplasm thickness to shrink from 155 nm to 125 nm (Figure S2) to cause the shift in the reflectance peak from 490 nm to 400 nm, as was observed between the light-adapted and the dark-adapted states.

To achieve such a decrease in *d*-spacing, the crystal platelets should change in orientation by 7°. However, because the (012) reflection was monitored rather than the platelet (102) reflection, the expected shift is reduced to an extent depending on the orientation of the (012) plane relative to the tilt direction. Accordingly, the maximum variation in the tilt angle observed in our experiments is about 3°. The crystal thickness used in previous models, >60 nm,[6a,10,12] is much larger than that measured here using cryo-SEM, 22 ± 4 nm. The cryo-SEM technique is very reliable in our opinion, because it enables direct measurements of the crystal thickness under conditions that are as close as possible to physiological conditions. Note that any mistake arising from the crystal fracture angle can only lead to an overestimation of the crystal thickness. The cryo-SEM technique also enables reliable measurements of the thickness of the cytoplasm layers after rapid freezing resulting in vitrification of the water. Information on cytoplasm thickness was previously not available. Consequently, cytoplasm thicknesses were inferred from a theoretical array structure that satisfied the constructive interference of the observed reflected color.

Lythgoe and Shand exposed the lateral stripe tissue to solutions of different osmotic pressure and obtained color changes. Based on this evidence they proposed that osmotically induced swelling and shrinking of the cells cause lateral movement of the crystals in a stack, without changing their orientation.[10,11c] In contrast, Nagaishi et al. and later Yoshioka et al. measured a change in crystal orientation after exposure of the tissue to elevated K^+ levels, which causes spectral transition to yellow, while keeping the osmotic pressure constant.[11a,b,12] None of the previous measurements was conducted on tissues exposed to direct light stimulation. After the dynamic, light-induced physiological measurements performed here, we can unequivocally conclude that the light-induced stimulus causes a reversible change in crystal orientation. It is however conceivable that the change in orientation is triggered by a change in tissue osmolarity.

While our results clearly demonstrate that the mechanism of the color change follows the "Venetian blinds" model, they do not identify the cellular machinery involved in control of the color change. Studies on the influence of neural inhibitors suggested that motor proteins and/or actin filaments play an important role in the system motility.[14] Further research is clearly needed to gain a more comprehensive understanding of the function of the cellular machinery in response to the changes in light stimulation.

The physical mechanism evolved by the neon tetra fish, produces tunable photonic crystals controlled by changing the tilt of the crystal arrays. Such light-triggered tunable systems are still out of reach in industrial materials. The insight gained from the neon tetra may thus provide inspiration for the design of optical applications such as in band-pass filters and in distributed Bragg reflectors. It can also conceivably inspire the development of novel materials in areas as diverse as paints and cosmetics in which guanine crystals are already in use.[15]

Keywords: biomineralization · guanine crystals · structural colors · tunable photonic crystals · X-ray diffraction

How to cite: *Angew. Chem. Int. Ed.* **2015**, *54*, 12426–12430
Angew. Chem. **2015**, *127*, 12603–12607

[1] J. W. Bradbury, S. L. Vehrencamp, *Principles of animal communication*, Sinauer, Sunderland, MA, **2011**.
[2] a) A. R. Parker, D. R. McKenzie, M. C. J. Large, *J. Exp. Biol.* **1998**, *201*, 1307–1313; b) A. R. Parker, *J. Opt. A* **2000**, *2*, R15–

R28; c) S. Kinoshita, S. Yoshioka, *ChemPhysChem* **2005**, *6*, 1442 – 1459.
[3] a) T. F. Anderson, A. G. Richards, *J. Appl. Phys.* **1942**, *13*, 748 – 758; b) H. Ghiradella, *Appl. Opt.* **1991**, *30*, 3492 – 3500.
[4] S. Vignolini, P. J. Rudall, A. V. Rowland, A. Reed, E. Moyroud, R. B. Faden, J. J. Baumberg, B. J. Glover, U. Steiner, *Proc. Natl. Acad. Sci. USA* **2012**, *109*, 15712 – 15715.
[5] L. Li, S. Kolle, J. C. Weaver, C. Ortiz, J. Aizenberg, M. Kolle, *Nat. Commun.* **2015**, *6*, 6322.
[6] a) E. J. Denton, M. F. Land, *Proc. R. Soc. London Ser. B* **1971**, *178*, 43 – 61; b) M. Land, *Prog. Biophys. Mol. Biol.* **1972**, *24*, 75 – 106; c) P. J. Herring, *Comp. Biochem. Physiol. Part A* **1994**, *109*, 513 – 546; d) J. Chae, S. Nishida, *Mar. Biol.* **1994**, *119*, 205 – 210; e) K. P. Mueller, T. Labhart, *J. Comp. Physiol. A* **2010**, *196*, 335 – 348; f) S. T. Rohrlich, R. W. Rubin, *J. Cell Biol.* **1975**, *66*, 635 – 645; g) D. Gur, Y. Politi, B. Sivan, P. Fratzl, S. Weiner, L. Addadi, *Angew. Chem. Int. Ed.* **2013**, *52*, 388 – 391; *Angew. Chem.* **2013**, *125*, 406 – 409.
[7] a) A. F. Huxley, *J. Exp. Biol.* **1968**, *48*, 227 – 245; b) S. Kinoshita, S. Yoshioka, J. Miyazaki, *Rep. Prog. Phys.* **2008**, *71*, 076401.
[8] a) A. Levy-Lior, B. Pokroy, B. Levavi-Sivan, L. Leiserowitz, S. Weiner, L. Addadi, *Cryst. Growth Des.* **2008**, *8*, 507 – 511; b) K. Guille, W. Clegg, *Acta Crystallogr. Sect. C* **2006**, *62*, o515 – o517.
[9] a) L. M. Mathger, M. F. Land, U. E. Siebeck, N. J. Marshall, *J. Exp. Biol.* **2003**, *206*, 3607 – 3613; b) K. Hiroaki, O. Noriko, F. Ryozo, *Comp. Biochem. Physiol. Part C* **1986**, *83*, 1 – 7; c) M. Goda, R. Fujii, *Zool. Sci.* **1998**, *15*, 323 – 333; d) J. Teyssier, S. V. Saenko, D. van der Marel, M. C. Milinkovitch, *Nat. Commun.* **2015**, *6*, 6368.
[10] J. N. Lythgoe, J. Shand, *J. Physiol.* **1982**, *325*, 23 – 34.
[11] a) H. Nagaishi, N. Oshima, R. Fujii, *Comp. Biochem. Physiol.* **1990**, *95*, 337 – 341; b) H. Nagaishi, N. Oshima, *Zool. Sci.* **1992**, *9*, 65 – 75; c) J. N. Lythgoe, J. Shand, *J. Exp. Biol.* **1989**, *141*, 313 – 325.
[12] S. Yoshioka, B. Matsuhana, S. Tanaka, Y. Inouye, N. Oshima, S. Kinoshita, *J. R. Soc. Interface* **2011**, *8*, 56 – 66.
[13] a) D. Gur, B. Leshem, D. Oron, S. Weiner, L. Addadi, *J. Am. Chem. Soc.* **2014**, *136*, 17236 – 17242; b) A. Levy-Lior, E. Shimoni, O. Schwartz, E. Gavish-Regev, D. Oron, G. Oxford, S. Weiner, L. Addadi, *Adv. Funct. Mater.* **2010**, *20*, 320 – 329.
[14] H. Nagaishi, N. Oshima, *Pigment Cell Res.* **1989**, *2*, 485 – 492.
[15] a) Z. Draelos, *Arch. Dermatol.* **2002**, *138*, 1262 – 1263; b) N. Delattre, L. Thevenet, Patent Application, WO2014097134A1, **2014**; c) S. Panush, J. M. Gelmini, European Patent Application, EP0439112A1, **1991**.

Received: March 11, 2015
Revised: April 13, 2015
Published online: April 27, 2015